

Why Precipitation Is Mostly Concentrated over Islands in the Maritime Continent

JIAN-HUA QIAN

International Research Institute for Climate and Society (IRI), Columbia University, Palisades, New York

(Manuscript received 12 February 2007, in final form 21 August 2007)

ABSTRACT

High-resolution observations and regional climate model simulations reveal that precipitation over the Maritime Continent is mostly concentrated over islands. Analysis of the diurnal cycles of precipitation and winds indicates that this is predominantly caused by sea-breeze convergence over islands, reinforced by mountain–valley winds and further amplified by the cumulus merger processes. Comparison of a regional climate model control simulation to a flat-island run and an all-ocean run demonstrates that the underrepresentation of islands and terrain in the Maritime Continent weakens the atmospheric disturbance associated with the diurnal cycle, and hence underestimates precipitation. The implication of these regional modeling results is that systematic errors in coarse-resolution global circulation models probably result from insufficient representation of land–sea breezes associated with the complex topography in the Maritime Continent. It is found that precipitation in the Maritime Continent, simulated by a global model, is indeed smaller than observed. The simulated upper-atmospheric velocity potential, which represents large-scale tropospheric heating, was substantially displaced eastward compared to observations. Possible approaches toward solving this problem are suggested.

1. Introduction

The Maritime Continent [a term coined by Ramage (1968), hereafter denoted by MC] consists of a multitude of large and small islands and seas off Southeast Asia. Many islands in the MC are mountainous (Fig. 1a). This paper analyzes regional climate processes associated with the diurnal cycles of precipitation and winds over the MC. Understanding of these small-scale processes is important for improving regional climate predictability, which is critical to the enhancement of modeling capability in local climate applications. The multiscale interaction between the diurnal cycle in the MC and large-scale processes also has an important implication for global atmospheric general circulation modeling, because the MC is situated at the core of the strongest monsoon region of the world, and its regional climate strongly influences both the Hadley and Walker circulations. Trade winds transport abundant moisture, collected from surface evaporation over the vast Pacific Ocean, toward the MC. Westerly winds over the Indian

Ocean also transport moisture toward the MC, particularly in spring and fall (Hastenrath and Lamb 2004; Wyrski 1973). The wind-driven ocean currents also bring warm tropical surface-layer waters toward the MC, forming a large area of warm water in the eastern Indian/western Pacific Ocean, called the warm pool. Evaporation from the warm pool increases atmospheric moisture in the region. Consequently, the region around the MC forms the largest rainy area on Earth, and the condensational latent heating released in precipitation processes drives the large-scale atmospheric circulation as a “boiler box” for the earth’s atmosphere (Simpson et al. 1993).

Most atmospheric general circulation models (GCMs) substantially underestimate precipitation over the MC (Neale and Slingo 2003). This may be because the grid resolution of these GCMs is too coarse to represent the complex topography over the MC. Indeed, the dimensions of some islands in the MC are only of the order of tens to a couple of hundred kilometers, that is, of subgrid scale to most coarse-resolution GCMs. Therefore, small-scale dynamics might be missing in coarse-resolution models. Due to their relatively small domain size, regional models can be run at a high enough resolution to study regional atmospheric processes without requiring excessive computational resources. In this paper, we will compare the results of a

Corresponding author address: Dr. Jian-Hua (Joshua) Qian, IRI, The Earth Institute at Columbia University, Lamont Campus, 61 Route 9W, Palisades, NY 10964-8000.
E-mail: jqian@iri.columbia.edu

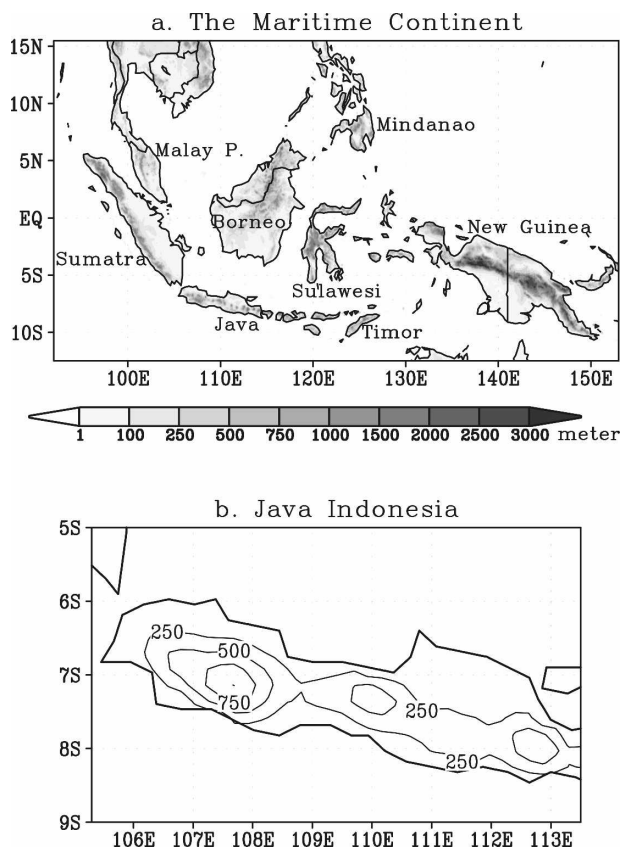


FIG. 1. (a) Topography of the Maritime Continent and (b) terrain heights over Java, Indonesia, as represented on the RegCM3 25-km grid (m).

30-yr simulation by a high-resolution regional climate model to satellite measurements.

Satellite precipitation estimates have the advantage of coverage over both land and sea. Their spatial and temporal resolutions have been greatly improved in recent years. We use NOAA/Climate Prediction Center's (CPC) Morphing Technique (CMORPH) 3-yr high-resolution observed precipitation dataset (Janowiak et al. 2005) to study regional precipitation processes in the MC from a climatological perspective. CMORPH combines the best features of measurements from geostationary and polar-orbiting satellites. The passive microwave rainfall estimates by polar satellites are more accurate than the infrared estimates by geostationary satellites. However, the geostationary satellites have higher space and time coverage. To achieve both accuracy and high spatial and temporal coverage, CMORPH uses the rainfall estimates derived from polar satellites, available at coarse resolution, then propagates these features in space using motion vectors derived from half-hourly geostationary satellite infrared data (Joyce et al. 2004; Dinku et al. 2007).

The diurnal cycles of wind systems are important in the tropics where synoptic-scale pressure gradients are weak, but local pressure gradients caused by differential solar radiative heating between different surface types (e.g., land versus sea, highland versus lowland) are strong. In the case of land-sea breezes, the land heats up rather quickly during the day under the influence of solar radiation, while sea surfaces remain cooler because the thermal inertia of water is relatively large and because waves, turbulence, and penetration into deep water mix heat downward from surface water. As a result, convective cells rise over land and sea breezes develop. At night, land cools off more rapidly than the ocean surface through longwave radiation loss, reversing the pressure gradients and forming land breezes. Similarly, in the case of mountain-valley winds, mountain slopes heat up rapidly due to solar radiation during a sunny day. The free atmosphere over valleys or lowlands remains less affected by solar insolation and is thus cooler than the air over mountain slopes. The warmer and lighter air over mountain slopes rises, inducing upslope valley winds and a compensating subsidence in the valley core (Rampanelli et al. 2004; Hughes et al. 2007; Prandtl 1952). At night, air over mountain slopes cools off faster than that over lowlands, resulting in downslope mountain winds. Land breezes (mountain winds) are usually weaker than sea breezes (valley winds) because the land-sea (mountain-valley) temperature difference due to daytime heating is much larger than that due to nighttime cooling. In mountainous coastal regions, land-sea breezes and mountain-valley winds, being roughly in phase with each other, may combine to strengthen the diurnal cycle of winds and form extended land-sea breezes, such as in the cases of the Yahagi River basin in Japan (Kitada and Igarashi 1986), Hong Kong (Wai et al. 1996), the Adriatic coast of Croatia (Nitis et al. 2005), and the Pacific coast of southern California (Hughes et al. 2007).

Land-sea breezes often play an important role in tropical precipitation. Pielke (1974) used a three-dimensional model to study the initiation and evolution of sea-breeze convergences over south Florida and found that the differential heating between land and water is the primary determinant of the magnitude of convergence, and that differential surface roughness indirectly influences convergence patterns through vertical turbulent transport of heat and momentum. Sea-breeze circulations affect the location of thunderstorm complexes over south Florida on undisturbed days. Pielke suggested that an understanding of the sea-breeze circulation is essential for interpreting the results of the Experimental Meteorology Laboratory's

cloud-merger seeding experiments over south Florida. Convection can be initiated ahead of sea-breeze fronts (Simpson et al. 1980; Fovell 2005). In a study of the cloud-seeding field experiments in Florida, Simpson et al. (1980) found that cloud-merger processes, in which small cumulus clouds merge to form larger and deeper ones to amplify precipitation, contributed to most of the convective rainfall. Simpson et al. (1993) found that cumulus mergers also play a major role in the almost daily development of a family of tall cumulonimbus complexes over a pair of flat islands (Bathurst and Melville Islands, collectively known as Tiwi Island) in the MC region north of Darwin, Australia, which were also studied in the Maritime Continent Thunderstorm Experiment (MCTEX; Keenan et al. 2000; Carbone et al. 2000). From satellite images over the MC region on 10 December 1978, Holland and Keenan (1980) noticed suppressed convection over land areas in the morning, but that convective clouds that developed in the afternoon mapped nearly perfectly onto every island and mountain range in the region. This afternoon convection provides a near-perfect map of the region; every island and mountain range is delineated by one or more cumulonimbi. By analyzing the European Union Cloud Archive User Service (CLAUS) data, Yang and Slingo (2001) found that afternoon rainfall is greater than morning rainfall over land, but less than morning rainfall over oceans throughout the tropics. The Tropical Rainfall Measuring Mission (TRMM) satellite measurements and rawinsonde sounding data revealed similar diurnal cycles of rainfall and convective intensity (Nesbitt and Zipser 2003; Mori et al. 2004).

Large-scale circulation also interacts with local land-sea breezes to affect the intensity and location of precipitation. Atkins and Wakimoto (1997) showed that sea-breeze fronts are stronger for offshore synoptic-scale flows than for parallel and onshore background flows. Sea-breeze directions may also change during the day depending on the shape of coastlines, the direction of large-scale winds, and the Coriolis effect (Simpson 1996). In studies of the Winter Monsoon Experiment (WMONEX) in the South China Sea, Houze et al. (1981) and Johnson and Priegnitz (1981) found that convergence between the winter monsoon and land breezes contributes to the nocturnal offshore rainfall northwest of Borneo. Mapes et al. (2003) found that gravity waves propagating from coastal mountains also play a role in developing nocturnal rainfall off the west coast of Colombia. Analysis of CLAUS data also showed that the strong diurnal signal over land is spread out over the adjacent oceans, probably through gravity waves (Yang and Slingo 2001).

In this paper, we investigate the physical mechanisms

for the spatial distribution of precipitation in the MC. The local precipitation processes associated with land-sea breezes are addressed, and their implications are discussed from a global climatological perspective. We will leave analyses of the role of the diurnal cycle in low-frequency climate variability for the future. Section 2 illustrates the characteristics of observed precipitation over the MC. Regional climate model results are analyzed in section 3, focusing on the Indonesian island of Java. Implications of the regional model results for global atmospheric modeling are discussed in section 4. Conclusions are drawn in section 5.

2. The spatial distribution of observed precipitation in the Maritime Continent

Figure 2 shows the 3-yr average (2003–05) of the CMORPH seasonal precipitation and the 30-yr climatology (1971–2000) of the National Centers for Environmental Prediction–National Center for Atmospheric Research (NCEP–NCAR) Reanalysis project (NNRP; Kalnay et al. 1996) seasonal 925-hPa winds and divergence. The monsoonal migration of precipitation is manifested in the MC. More precipitation falls over the southern MC in the boreal winter months of December–February (DJF), with more rainfall in the northern MC in the boreal summer months of June–August (JJA) and with intermediate values during the boreal spring (March–May, or MAM) and fall (September–November, or SON).

In addition to the monsoonal effect, the high-resolution (0.25° grid) satellite data reveals the inhomogeneity in the spatial distribution of precipitation, with a strong contrast between land and sea, over the MC in all seasons. Heavy precipitation is concentrated over the islands with a relatively dry ring surrounding each island. Even during the dry season in the southeastern area of the MC, such as over Timor Island, we can still see slightly more rainfall over the islands than over the surrounding seas. There are also secondary heavy precipitation belts located in the middle of the seas between large islands, for example, in the Java Sea between the islands of Java and Borneo in DJF, MAM, and SON. Precipitation data from the TRMM (Kummerow et al. 2000; Nesbitt and Zipser 2003) also share similar spatial features. Low-level horizontal divergence calculated from NNRP winds (on $2.5^\circ \times 2.5^\circ$ grids) shows that mesoscale convergence centers are coincident with two large precipitation centers, one over Borneo and another over Sumatra/Malay Peninsula, but in between is an area of relatively weak convergence (in SON and DJF) or divergence (in JJA and MAM). Hence, the effect of a heterogeneous distribu-

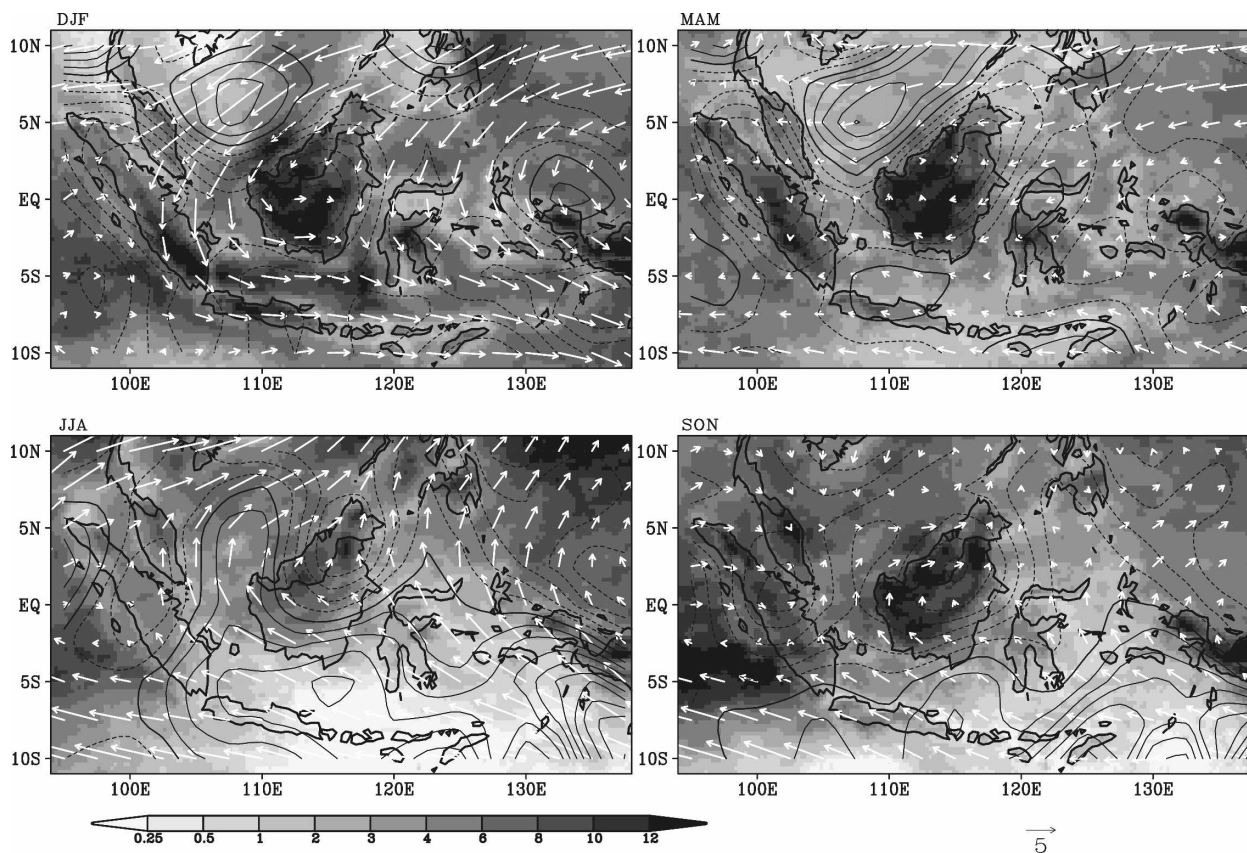


FIG. 2. Averaged (2003–05) CMORPH seasonal precipitation (mm day^{-1} , shaded), and climatology (1971–2000) of the NNRP horizontal winds (vectors) and divergence (contours) at 925 hPa over the MC.

tion of rainfall is somewhat captured even by the coarse-grid winds. However, the coarse-grid winds cannot explain the finescale distribution of rainfall, such as over Java and Sulawesi.

It is well known that diurnal cycles of temperature, rainfall, and winds are more pronounced in the tropics than in the extratropics (Riehl 1954). Due to the smaller heat capacity of land compared to that of the ocean, the amplitude of the diurnal cycle of the surface and lower-atmospheric temperature over land is much larger than that over the ocean (Webster et al. 1996). The land–sea breezes resulting from the local temperature and pressure gradients may cause finescale rainfall differences between land and sea. Figure 3 shows the diurnal cycle of rainfall over Borneo, the Java Sea, and the Java, based on the 3-hourly rain rate from the CMORPH satellite rainfall estimation. The magnitude of the diurnal cycle is largest in the DJF wet season, followed by MAM and SON (not shown), and smallest in the JJA dry season. The magnitude of the diurnal cycle over Java is very strong in DJF, with a maximum rain rate of about 25 mm day^{-1} in the afternoon during the 3-h period from 1600 to 1900 LT (or around 1730

LT, where LT denotes the local standard time of Jakarta, Indonesia, UTC +7 h). The diurnal cycle over Borneo is also quite strong, with similar magnitude in all seasons except JJA. The phase of the diurnal cycle of rainfall over Borneo is different from that over Java, with heavy rainfall lasting longer, to midnight and early morning. TRMM satellite rainfall measurements show that, although rainfall from small- or medium-sized clouds ends earlier in the afternoon, mesoscale convective systems developed during the afternoon and maintained their strength until early morning over Borneo (Nesbitt and Zipser 2003). Ichikawa and Yasunari (2006) also observed leeward propagation of rainfall activity in the TRMM Precipitation Radar data. Over the Java Sea, between the two large islands, the diurnal cycle is very strong in DJF but is weakened in other seasons. The phase over the sea is roughly opposite that over Java. Off the south coast of Java in the Indian Ocean (not shown), there also exists a diurnal cycle, but its magnitude is smaller than that off the north coast, over the Java Sea. As we will see later, precipitation over the Java Sea is affected by land breezes from both Borneo and Java, which strengthen the diurnal cycle. In

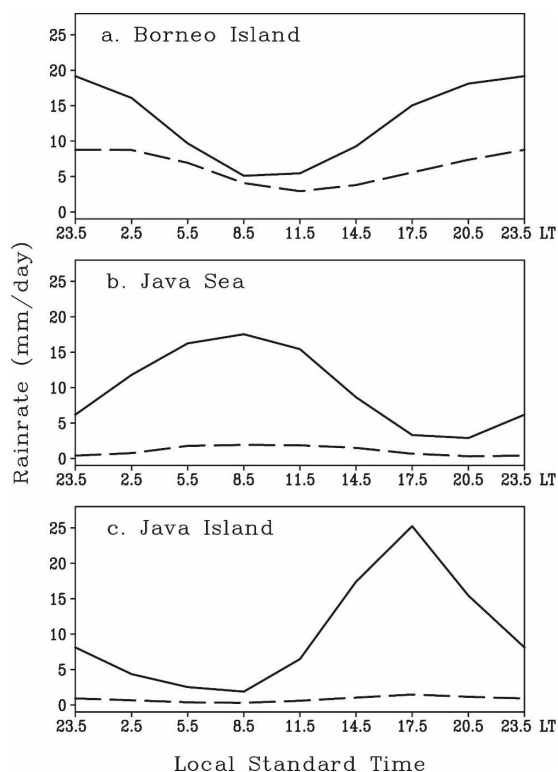


FIG. 3. The mean diurnal cycle of CMORPH observed rain rate (mm day^{-1}) in DJF (solid) and JJA (dashed), averaged in a rectangular area of (a) 2°S – 1°N , 111° – 116°E over Borneo, (b) 5.5° – 4.5°S , 107° – 112°E over the Java Sea, and (c) 7.7° – 6.7°S , 107° – 112°E over the island of Java. The local standard time is denoted by LT.

contrast, the region off the south coast only has land breezes from Java.

To examine the spatial pattern of diurnal rainfall evolution over the MC, the averaged diurnal cycle of the 3-hourly CMORPH precipitation in DJF (mean of 271 days) is shown in Fig. 4. As is common for the whole MC region, the diurnal cycle of precipitation is found to be pronounced not only over islands, but also over the seas between large islands, with smaller magnitude and roughly opposite phase over the seas compared to over the islands. Precipitation over islands reaches a maximum in late afternoon/evening and a minimum at night/early morning. In contrast, precipitation over the seas is maximum at night/early morning and light during afternoon/early evening. Rainfall usually occurs earlier near the coast, gradually propagating inland. Therefore, some coastal areas, such as Jakarta, may experience morning rain, while rainfall maxima reach inland in the afternoon. The phase of the diurnal cycle also depends on the size of the islands. In small or narrow islands (such as Java, Timor, Sulawesi), precipitation reaches a maximum early in the afternoon,

around 1300–1900 LT. In medium-sized islands, such as Sumatra, precipitation reaches a maximum later, around 1600–2100 LT. But for the large island of Borneo, precipitation reaches a maximum even later, at night, 1900–0100 LT, as is also shown in the TRMM data by Nesbitt and Zipser (2003).

To further illustrate the diurnal cycle, a blown-up figure of precipitation over Java, with its daily mean removed to highlight the diurnal cycle, is shown in Fig. 5. The positive phase of precipitation over land persists during 1300–2200 LT but over the ocean it is during 0100–1300 LT, lasting a little longer than over land. Figure 3 reveals that precipitation over land during the afternoon hours is quite heavy. Precipitation starts to move away from the island toward the surrounding seas in 2200–0100 LT, with some precipitation near the coastlines, particularly near a bay with concave coastlines from 108° to 110°E , where land breezes converge off the coast. Gradually moving away from the island, the precipitation area reaches farthest seaward during 1000–1300 LT.

The strong contrast in precipitation between land and sea indicates possible roles of land–sea breezes in maintaining the precipitation distribution. Because the observational data of finescale and high-frequency winds over both land and sea are not available, we use a regional climate model to generate winds and study the role of the diurnal cycle in precipitation in the next section.

3. The diurnal cycle over Java as simulated by a regional climate model

Diurnal cycles of rainfall and winds are analyzed in a 30-yr, 25-km grid regional climate model simulation over Java. The model is the Abdus Salam International Centre for Theoretical Physics (ICTP) Regional Climate Model version 3 (RegCM3; Giorgi et al. 1993; Giorgi et al. 2006), a mesoscale model based on atmospheric primitive equations. The radiation parameterization scheme in RegCM3 is adopted from the Community Climate Model version 3 (CCM3; Kiehl et al. 1998). An explicit moisture scheme is used for resolved (grid scale) precipitation (Pal et al. 2000). The subgrid-scale cumulus convection scheme is that of the Emanuel–Massachusetts Institute of Technology (MIT) scheme (Emanuel and Zivkovic-Rothman 1999). The regional model is driven by lateral boundary conditions provided by the NCEP–NCAR reanalysis (Kalnay et al. 1996). The regional model is also forced by the underlying lower boundary of the land and ocean surfaces. Over land area, the Biosphere Atmosphere Transfer

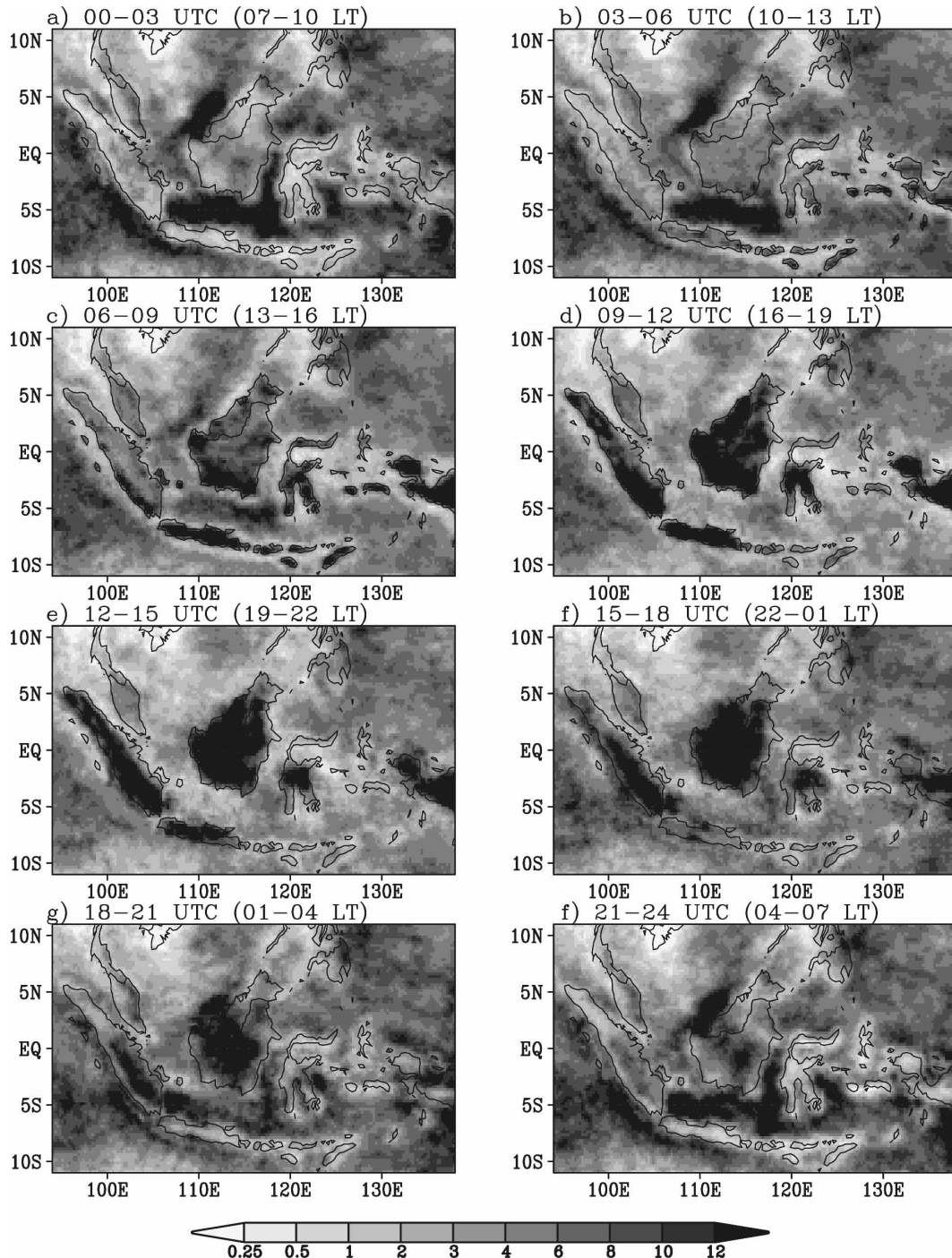


FIG. 4. Diurnal cycle of CMORPH precipitation (mm day^{-1}) in DJF in the MC. The local standard time is denoted by LT (UTC + 7 h).

Scheme (BATS; Dickinson et al. 1993) is employed to compute surface radiative, sensible and latent heat, and momentum fluxes and surface temperature based on the assigned vegetation and soil parameters. Over the ocean, the model is forced by sea surface temperatures

(SSTs) spatially and temporally interpolated from a monthly dataset. Therefore, there is no diurnal variation in the prescribed SST field. Since sea breezes are mostly caused by the strong diurnal cycle of temperature over land, and the observed diurnal cycle of SST is

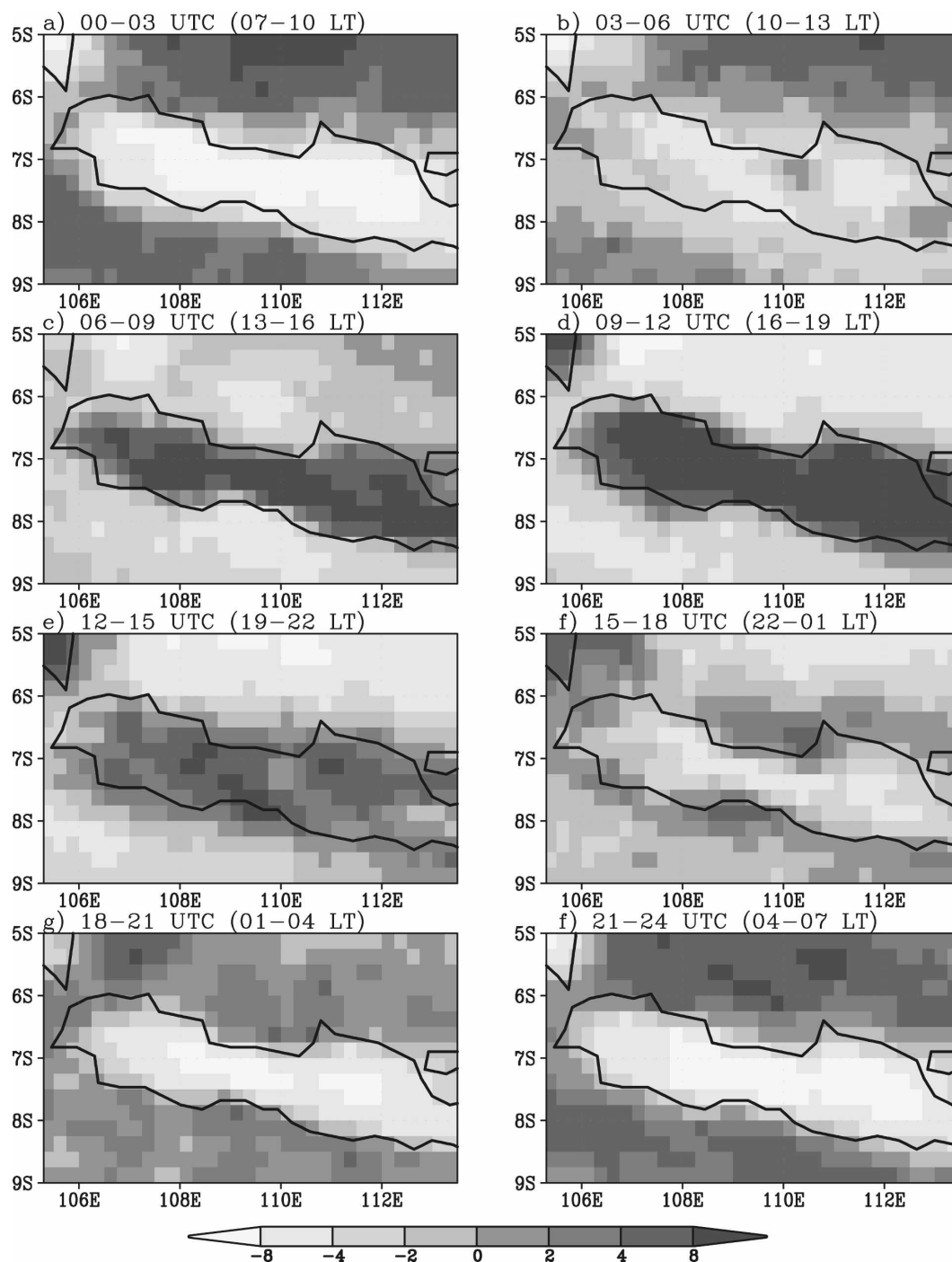


FIG. 5. Diurnal cycle of CMORPH precipitation (mm day^{-1}) over Java in DJF. Daily means are subtracted to highlight the diurnal cycle.

rather small (Webster et al. 1996), using the prescribed SST in this study should not seriously affect the results.

The terrain over Java represented by the 25-km-grid RegCM3 is shown in Fig. 1b. The island is elongated roughly in the east–west direction with a slightly north–

west–southeast tilt. A chain of mountains with several peaks runs along the narrow island. The north–south width of the island is about 1° – 2° of latitude. The coastline is also curved, for example, concave along both north and south coasts between 108° and 110°E .

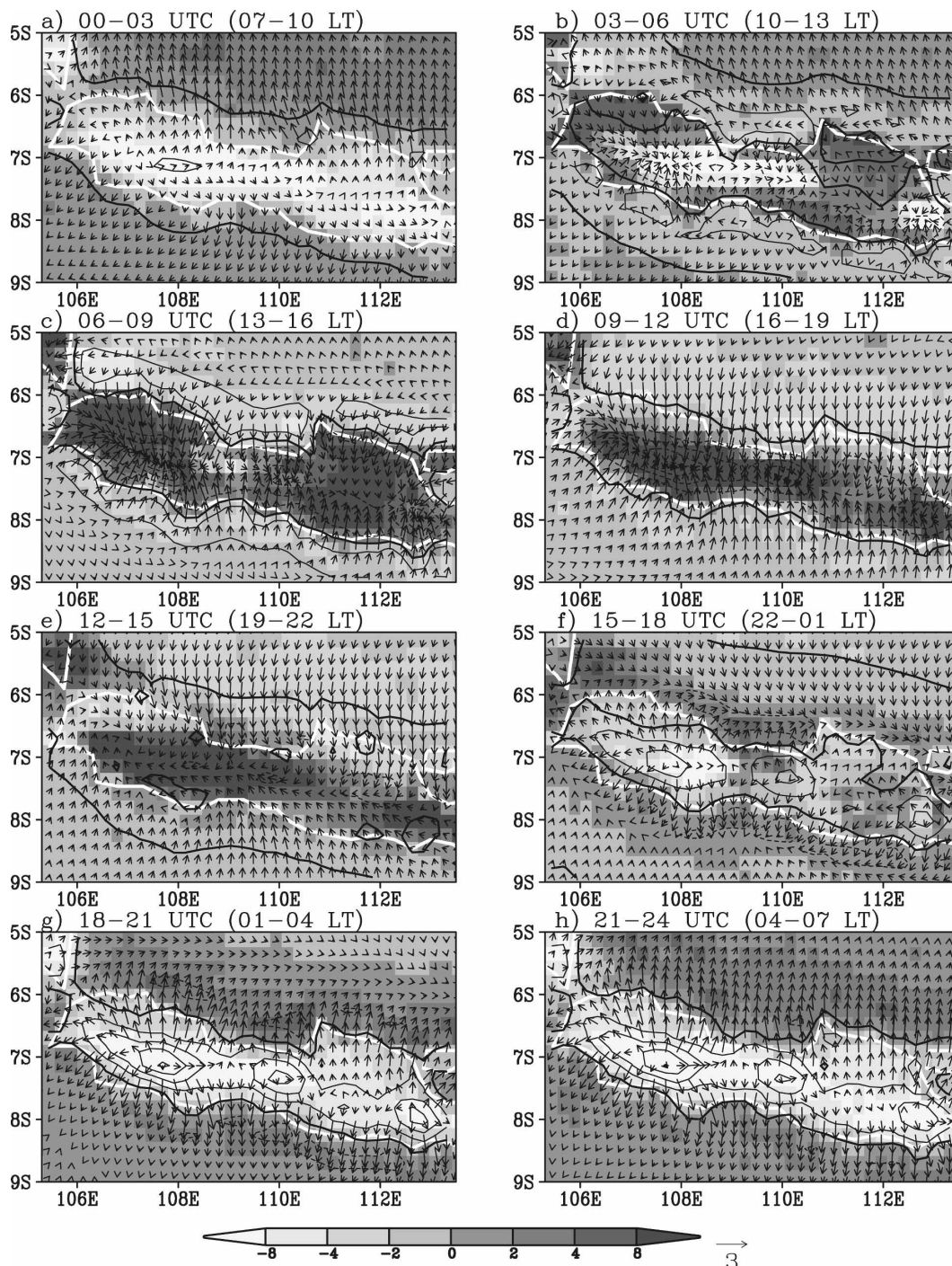


FIG. 6. Climatology (1971–2000) of the diurnal cycle of NNRP-driving RegCM3 precipitation (mm day^{-1} , shaded), horizontal winds (m s^{-1} , vectors), and divergence (contour interval is $2 \times 10^{-5} \text{ s}^{-1}$, zero-divergence lines are thick solid) at 10-m height in DJF. Daily means are subtracted to highlight the diurnal cycle. Coastlines are white.

Figure 6 shows the simulated mean diurnal cycles of precipitation, horizontal winds, and divergence at 10-m height in DJF (averaged over 30 years from 1971 to 2000, a total of 2708 days). To highlight the diurnal

cycle, daily means are subtracted in the figure. Compared to the observations in Fig. 5, the diurnal cycle of precipitation is well simulated. In the morning hours after sunrise (0700–1000 LT, top-left panel), land

breezes still prevail as in the early morning before sunrise (bottom two panels). During late morning (1000–1300 LT; top right panel in Fig. 6), winds over the seas are still in the direction of the land breeze, but winds near the mountains over Java start to converge toward the mountain peaks, located at about (7°S , 107.5°E), (7.5°S , 110°E), and (8°S , 113°E), in the form of valley winds; therefore, divergence and a dry ring show up over the coastal seas. Sea breezes blow toward Java from early afternoon to late evening (1300–2200 LT). Sea-breeze convergences enhance a large amount of precipitation over Java during this period. Around midnight (2200–0100 LT), winds over the seas are still in the direction of sea breezes, but winds near the mountains start to diverge away from the peaks as mountain winds; consequently, convergence and a wet ring form around the island. Wet areas also form in the valleys between the mountain peaks on the island. The daily wind anomalies reverse direction after midnight and become land breezes and mountain winds during the morning hours (0100–1000 LT), lasting until after sunrise. Mountain–valley winds respond more swiftly to insolation than land–sea breezes do. Thus, the phase of the former is slightly ahead of the latter. The spatial scale of the breezes should be in accordance with their forcings, respectively; that is, mountain–valley winds should be of mountain scale, which is smaller than island scale, as will be seen in the next figure, which describes mountain effects.

To distinguish the impact of mountains from that of the land–sea contrast on the diurnal cycle, a version of RegCM3 with a flat-island of uniform 1.5-m height (TER) is run. The pattern of the diurnal cycle of land–sea breezes in the TER run (not shown) is generally similar to, but a little weaker than, that in the mountainous control run (CTL). Compared to CTL, the timing of rainfall development over Java starts 3 h earlier (1000–1300 LT) in TER, probably due to faster penetration of sea breezes over the smooth flat island, and the large precipitation also ends 3 h earlier (1600–1900 LT) in TER (also see Fig. 8). To examine the evolution of the net effect of mountains during the diurnal cycle, the differences (CTL minus TER) of the climatologies of rainfall and winds in each 3-h time bin are calculated and shown in the eight panels of Fig. 7. Precipitation differences over Java between the two runs are positive during the sea breeze hours of 1300–0100 LT, but mostly negative during the land breeze hours of 0700–1300 LT. This means that the mountains work to enhance the diurnal cycle of precipitation. The mountain–valley winds with opposite wind direction between day and night are manifested in Fig. 7, as well as in Fig. 6. Right after sunrise (0700–1000 LT, Fig. 7a), conver-

gences of valley winds are initiated in the vicinity of the three mountain peaks. During 1000–1300 LT, in late morning and near noon (Fig. 7b), valley-wind convergences expand to larger areas, but enhanced precipitation over most of the central mountain range does not begin until later, except for over the two small mountains at about (7.5°S , 110°E) and (8°S , 113°E). In the early afternoon (1300–1600 LT), the CTL run produces more (less) rainfall over the mountain peaks (coastlands) than for the TER run. The large positive precipitation difference in the afternoon (1600–2200 LT) over the central mountain range indicates that valley winds enhance the diurnal cycle greatly and help to concentrate more rainfall over the mountains. Around midnight (2200–0100 LT) and afterward, although the mountain winds diverge from the mountain peaks, positive precipitation differences are still widespread over most of the areas of the island and adjacent ocean. The combined sea breezes and valley winds enlarge rainfall over Java, particularly over the mountain range, and energize it to last longer into the evening.

A considerable amount of precipitation over Java in the CTL run (as well as in the CMORPH observation) persists after sunset (Figs. 4e, 5e, 6e, and 7e). This fact indicates that the “cumulus merger” process is also at work here, similar to that over Florida (Simpson et al. 1980) and Tiwi Island north of Australia (Simpson et al. 1993; Saito et al. 2001). Once the sea breezes and valley winds converge over the island to initiate precipitation, the self-amplifying cumulus merger process takes over to maintain precipitation until midnight. Deep convection associated with the cumulus merger is, however, strongly controlled by large-scale atmospheric conditions. For example, during the dry season in the small islands of the southeastern MC, such as over Timor, heavy precipitation is prohibited, even though they are surrounded by vast warm seas where low-level moisture should not be lacking (Fig. 1). This fact indirectly proves the importance of cumulus merger in amplifying precipitation initiated by sea-breeze convergence.

Figure 8 shows the timing and intensity of the mean diurnal cycle of the rain rate simulated by the RegCM3 control run averaged in the rectangular area of (7.7° – 6.7°S , 107° – 112°E) over Java in DJF. The corresponding observed diurnal cycle of the CMORPH precipitation is also shown for reference; it is well reproduced by RegCM3 in terms of both phase and magnitude. The near-surface air temperature over Java (not shown) reaches its daily maximum in early afternoon, at about 1300 LT. But the precipitation maximum occurs about 5 h later, around sunset. The peak rain rate reaches over 20 mm day^{-1} . Such a large rain rate must result from heavy rainfall associated with deep convection.

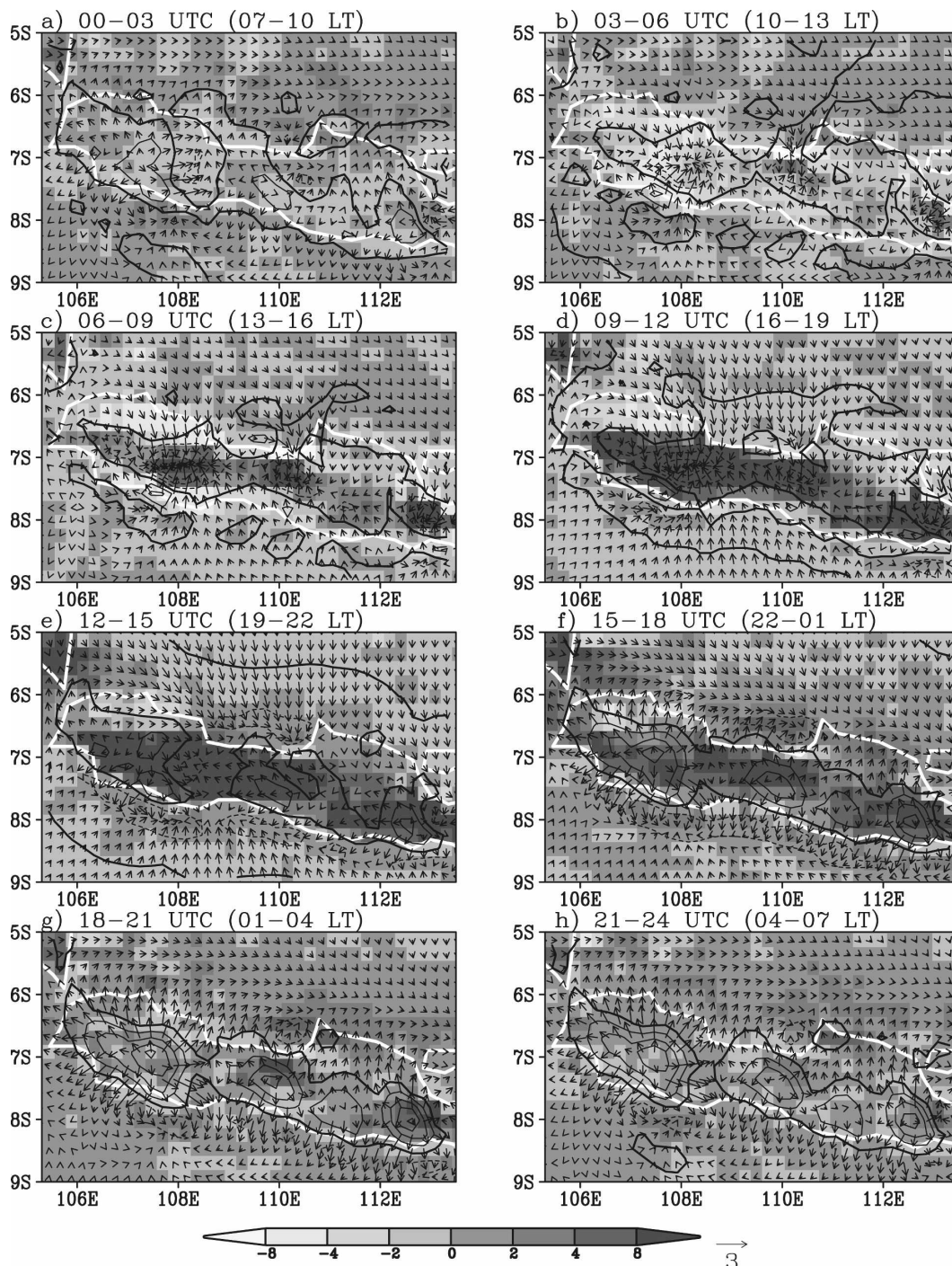


FIG. 7. Difference, over a diurnal cycle, between the RegCM3 control run and a flat-island run (CTL – TER) in precipitation (mm day^{-1} , shaded), horizontal winds (m s^{-1} , vectors), and divergence (the contour interval is $2 \times 10^{-5} \text{ s}^{-1}$, zero-divergence lines are thick solid) at 10-m height in DJF. Coastlines are white. The diagram shows net mountain effects on the diurnal cycles of winds and precipitation.

Deep convective clouds, called hot towers by Riehl and Malkus (1958), are instrumental for transporting heat from the planetary boundary layer to the upper troposphere (Hartmann et al. 1984; Tao et al. 2006). The

diurnal cycle of the rain rate in the flat-island run is also plotted for comparison. Without mountains, the rainfall intensity during the day is significantly reduced, and the timing of the maximum rainfall also comes earlier.

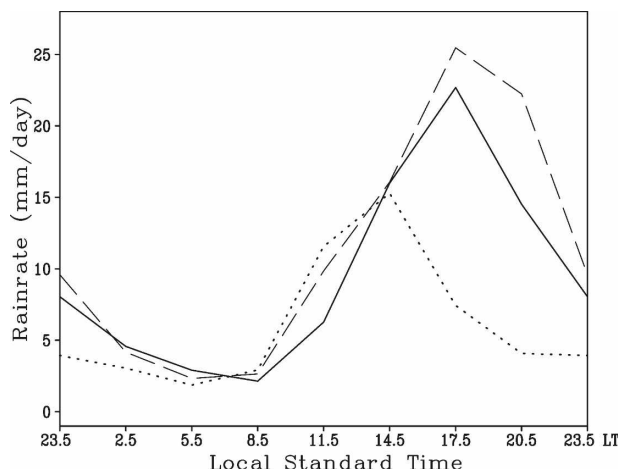


FIG. 8. The DJF mean diurnal cycles of the CMORPH observed rainfall (mm day^{-1} , solid) and RegCM3 simulated rainfall (mm day^{-1}) in the mountainous control run (dashed) and a flat-island run (dotted), spatially averaged in a rectangular area of 7.7° – 6.7°S , 107° – 112°E over Java.

In summary, as shown by Figs. 6–8, during daytime, sea-breeze fronts from both north and south coasts converge over the middle of the island, are reinforced by the convergence of valley winds near the mountaintops, form an elongated low-level convergence line, and trigger moist convection over Java, where plenty of moisture is readily available to fuel heavy precipitation.

Similar occurrences of sea-breeze convergence should also take place over other islands in the MC. For an elongated narrow island such as Java or Sumatra, two parallel lines of sea-breeze fronts from opposite coasts converge to form a precipitation belt along the island. Over other islands, regardless of shape, sea breezes from surrounding seas converge toward the center of each island and produce ascent and precipitation over the island during afternoon and evening hours. For example, over the large island of Borneo, rainfall is observed to be initiated along the sea-breeze front along the coastlands during 1300–1600 LT, but takes a relatively long time to collide at the center of the island, which happens late in the evening (Figs. 3 and 4). For small islands, it only takes a short time for the sea breezes to collide; therefore, maximum rainfall is reached in the early afternoon (Fig. 4). Since many islands in the MC are mountainous, valley winds reinforce sea breezes to enhance precipitation over the islands. Then, self-amplification by cumulus mergers intensify precipitation. This explains why the observed precipitation is mostly concentrated over the islands in the MC and why precipitation is usually larger over the mountains than over the flat coastlands.

Late at night and during morning hours, the land

surface cools down, and low-level winds reverse direction, becoming land breezes. Owing to the complex network of islands of the MC, land breezes from neighboring islands converge toward the middle of the seas between them at night and form nocturnal precipitation over the sea. Although the diurnal cycle of atmospheric temperature over the sea is relatively small, the land-breeze convergence still generates a secondary heavy rain belt over the sea during the night and morning, as observed in Figs. 2–4. Here, gravity waves may also play a role in spreading the diurnal signal over land out to the adjacent oceans, as noted by Yang and Slingo (2001) and Mapes et al. (2003).

On a seasonal time scale, the interaction of the monsoon with topography also affects local precipitation (Chang et al. 2005). Land–sea breezes also interact with large-scale winds (Ichikawa and Yasunari 2006).

The major large-scale atmospheric moisture source is evaporation from subtropical oceans (Trenberth 1999). Then the moisture is transported to remote places in the tropics by winds (Hastenrath and Lamb 2004). Therefore, from a global perspective, the combination of islands and seas in the MC is optimally located to accumulate the incoming moisture from the oceans transported by the trade winds, assisted by the day and night alternation of land–sea breezes and mountain–valley winds, to produce huge amounts of precipitation and latent heating of the atmosphere.

4. Implications of the role of the diurnal cycle for large-scale atmospheric modeling

The regional modeling results discussed above indicate that, in order to simulate diurnal cycles, the islands and terrain of the MC must be sufficiently represented in numerical models. Otherwise, atmospheric disturbances associated with the diurnal cycle of land–sea and mountain–valley winds are reduced and precipitation is underestimated. To confirm this point, we ran a version of RegCM3 (SEA) in which the island of Java was removed and replaced by sea. Then, the total precipitation in the model domain was compared to that in the control run (CTL) and the flat-island run (TER) as an extreme case of underestimation of mountain heights (Fig. 9). As expected, the TER run produced less precipitation than for the CTL run, indicating that precipitation is underestimated if mountain height is underestimated, as in coarse-resolution models. The SEA run produced even less rainfall than the TER run, indicating that the neglect of small islands further reduces precipitation.

As a consequence of underestimating precipitation over the MC, the condensational latent heating in the atmosphere is decreased, which further affects the gen-

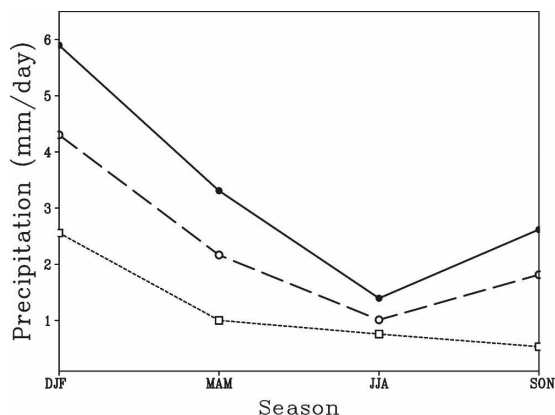


FIG. 9. Climatology (1971–2000) of seasonal precipitation (mm day^{-1}) averaged over Java and the adjacent ocean in the domain of 9° – 5° S, 105.5° – 113.5° E for the RegCM3 control run (solid), a flat-island run (long dashes), and an all-ocean run (short dashes).

eral circulation of the atmosphere. Many GCMs have difficulty simulating the Asian monsoon and tend to underestimate precipitation over the MC (Gadgil and Sajani 1998; Neale and Slingo 2003). Figure 10c shows an example of a GCM simulation with ECHAM4.5 (Roeckner et al. 1996) at T42 resolution (corresponding to a 2.8125° grid). The observed climatology (1982–2002) of NOAA's Climate Prediction Center Merged Analysis of Precipitation (CMAP; Xie and Arkin 1996) and NNRP velocity potential (Φ , defined by $\nabla\Phi = -\mathbf{V}$, where \mathbf{V} is the horizontal velocity) at 200 hPa are shown in Fig. 10a. Maximum precipitation covers the MC and the rest of the warm pool region. The minimum 200-hPa velocity potential (roughly corresponding to the maximum tropospheric heating) is directly over the MC. The land–sea masks in the ECHAM4.5 model at T42 resolution are shown in Fig. 10b. Large islands (such as Borneo) are underrepresented, and medium and small islands (such as Java and Timor) are not represented at all. In the GCM results (Fig. 10c), precipitation over the MC is underestimated compared to the CMAP data, and the minimum velocity potential center is displaced eastward by more than 2000 km. Hoerling et al. (1992) reported similar climate drift in the NCAR Community Climate Model (CCM1) simulations. Because of the role of the atmospheric heating over the MC as an important energy source for the large-scale circulation, the systematic error in precipitation over the MC will inevitably contaminate simulations elsewhere, such as in the Asian–Australian monsoon, subtropical jets, and storm tracks.

5. Discussion and conclusions

CMORPH data reveal that precipitation in the MC is mostly concentrated over islands in the afternoon and

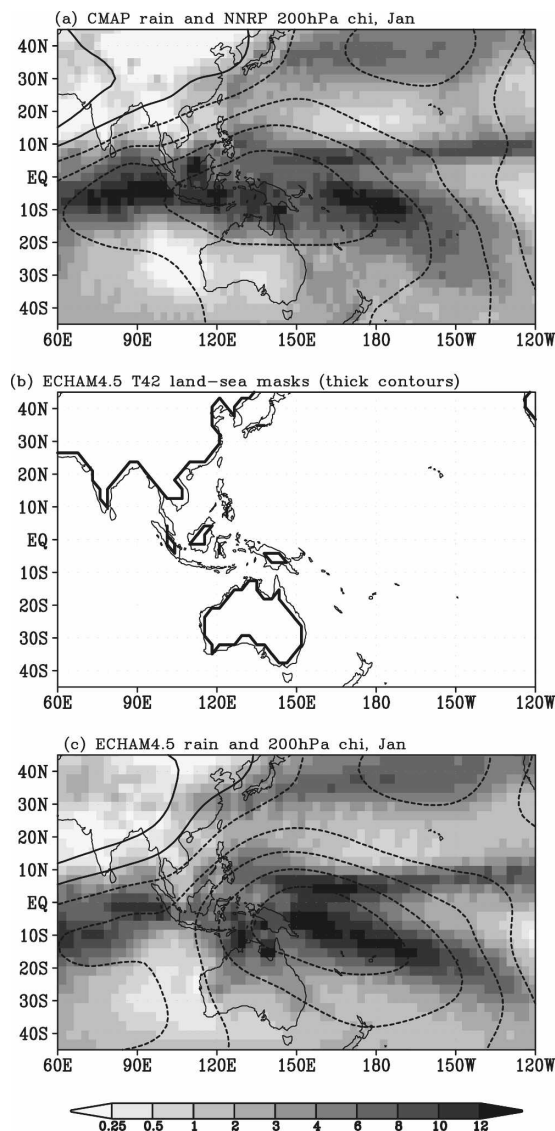


FIG. 10. (a) Climatology (1982–2002) of the observed CMAP monthly precipitation (mm day^{-1} , shaded), and NNRP 200-hPa velocity potential (contour interval of $1 \times 10^6 \text{ m}^2 \text{ s}^{-1}$). (b) Land–sea masks in the ECHAM4.5 T42 model (thick contours). (c) Climatology (1982–2002) of the simulated ECHAM4.5 precipitation (mm day^{-1} , shaded) and 200-hPa velocity potential (contour), which is displaced eastward compared to that in (a).

evening, with a secondary concentration of rainfall over the seas between large islands during late night and morning hours. We have shown that the diurnal cycle of winds has a major role in maintaining the spatial distribution of precipitation. Results from regional climate model simulations suggest the following explanations:

- (i) During daytime, because solar radiation more effectively heats the islands than the seas, sea breezes are initiated.

- (ii) Sea-breeze fronts converge from the coasts toward the center of each island in the afternoon, lift moist air, and trigger convection.
- (iii) Valley winds reinforce sea breezes, enhancing convergence over mountainous islands.
- (iv) Cumulus merger processes take over to further enhance precipitation.

Similarly, land-breeze convergence contributes to the less heavy nocturnal and morning rainfall over the seas.

The above analysis suggests that underestimation of precipitation over the MC in coarse-resolution GCMs probably results from the underrepresentation, or even absence, of islands and mountains, thus weakening the atmospheric disturbance caused by the daily alternation of land-sea breezes and mountain-valley winds. Since the latent heating over the MC works as a “boiler box” for the atmosphere, systematic errors in this region may seriously affect the global circulation.

To reduce systematic errors, it is crucial to enhance the spatial resolution over the MC in numerical models. One approach is to use multiscale unified models, as proposed by Semazzi et al. (1995) and Qian et al. (1998), among others. These models are being developed at major research centers such as the Met Office’s Hadley Centre (Johns et al. 2006) and the Japanese Earth Simulator (Sato 2004). But running a global model at high resolution is computationally very expensive, especially for long-term climate simulations. Another approach is to use a two-way nesting, stretched-grid regional model that concentrates high resolution over the area of interest (Qian et al. 1999), or interactively nesting a fine-grid regional model into a coarse-grid global model (Lorenz and Jacob 2005).

It should be noted that we only focused on the climatology of the diurnal cycle and its role in the spatial distribution of precipitation over the MC. Other important issues of multiscale interaction between the diurnal cycle and longer-term weather and climate variations, such as monsoon surges and lulls, intraseasonal oscillation, and ENSO, warrant further investigation.

Acknowledgments. I wish to thank Filippo Giorgi, Xunqiang Bi, Jeremy Pal, Sara Rauscher, and other members of the Abdus Salam ICTP Physics for Weather and Climate Group, the developers of RegCM3. The Max Planck Institute for Meteorology (Hamburg, Germany) kindly made the ECHAM4.5 model available to the International Research Institute for Climate and Society (IRI) at Columbia University. I also thank Huilan Li for programming support; David DeWitt for providing the ECHAM4.5 data; Esther Ebrahimi, Tufa Dinku, and Shiv Someshwar for valu-

able discussions; and Chester Ropelewski, Lareef Zubair, Andrew Robertson, Alessandra Giannini, and James Hansen for reading the manuscript and providing helpful suggestions. Constructive suggestions by the editor and two anonymous reviewers helped to improve the manuscript greatly. This paper is funded by a grant/cooperative agreement from the National Oceanic and Atmospheric Administration, NA05OAR4311004. The views expressed herein are those of the author and do not necessarily reflect the views of NOAA or any of its subagencies.

REFERENCES

- Atkins, N. T., and R. M. Wakimoto, 1997: Influence of the synoptic-scale flow on sea breezes observed during CaPE. *Mon. Wea. Rev.*, **125**, 2112–2130.
- Carbone, R. E., J. W. Wilson, T. D. Keenan, and J. M. Hacker, 2000: Tropical island convection in the absence of significant topography. Part I: Life cycle of diurnally forced convection. *Mon. Wea. Rev.*, **128**, 3459–3480.
- Chang, C.-P., Z. Wang, J. McBride, and C. Liu, 2005: Annual cycle of Southeast Asia–Maritime Continent rainfall and the asymmetric monsoon transition. *J. Climate*, **18**, 287–301.
- Dickinson, R. E., A. Henderson-Sellers, and P. J. Kennedy, 1993: Biosphere Atmosphere Transfer Scheme (BATS) version 1e as coupled to the NCAR Community Climate Model. NCAR Tech. Note NCAR/TN-387+STR, 72 pp.
- Dinku, T., P. Ceccato, E. Grover-Kopec, M. Lemma, S. J. Connor, and C. F. Ropelewski, 2007: Validation of satellite rainfall products over East Africa’s complex topography. *Int. J. Remote Sens.*, **28**, 1503–1526.
- Emanuel, K. A., and M. Zivkovic-Rothman, 1999: Development and evaluation of a convective scheme for use in climate models. *J. Atmos. Sci.*, **56**, 1766–1782.
- Fovell, R. G., 2005: Convective initiation ahead of sea-breeze front. *Mon. Wea. Rev.*, **133**, 264–278.
- Gadgil, S., and S. Sajani, 1998: Monsoon precipitation in the AMIP runs. *Climate Dyn.*, **14**, 659–689.
- Giorgi, F., M. R. Marinucci, and G. T. Bates, 1993: Development of the second-generation Regional Climate Model (RegCM2). Part I: Boundary-layer and radiative transfer processes. *Mon. Wea. Rev.*, **121**, 2794–2813.
- , J. S. Pal, X. Bi, L. Sloan, N. Elguindi, and F. Solmon, 2006: Introduction to the TAC special issue: The RegCM2 network. *Theor. Appl. Climatol.*, **86**, 1–4.
- Hartmann, D. L., H. H. Hendon, and R. A. Houze Jr., 1984: Some implications of the mesoscale circulations in tropical cloud clusters for large-scale dynamics and climate. *J. Atmos. Sci.*, **41**, 113–121.
- Hastenrath, S., and P. J. Lamb, 2004: Climate dynamics of atmosphere and ocean in the equatorial zone: A synthesis. *Int. J. Climatol.*, **24**, 1601–1612.
- Hoerling, M. P., M. L. Blackmon, and M. Ting, 1992: Simulating the atmospheric response to the 1985–87 El Niño cycle. *J. Climate*, **5**, 669–682.
- Holland, G. J., and T. D. Keenan, 1980: Diurnal variations of convection over the “Maritime Continent.” *Mon. Wea. Rev.*, **108**, 223–225.
- Houze, R. A., Jr., S. G. Geotis, F. D. Marks Jr., and A. K. West, 1981: Winter monsoon convection in the vicinity of north

- Borneo. Part I: Structure and time variation of clouds and precipitation. *Mon. Wea. Rev.*, **109**, 1595–1614.
- Hughes, M., A. Hall, and R. G. Fovell, 2007: Dynamical controls on the diurnal cycle of temperature in complex topography. *Climate Dyn.*, **29**, 277–292.
- Ichikawa, H., and T. Yasunari, 2006: Time–space characteristics of diurnal rainfall over Borneo and surrounding oceans as observed by TRMM-PR. *J. Climate*, **19**, 1238–1260.
- Janowiak, J. E., V. E. Kousky, and R. J. Joyce, 2005: Diurnal cycle of precipitation determined from the CMORPH high spatial and temporal resolution global precipitation analyses. *J. Geophys. Res.*, **110**, D23105, doi:10.1029/2005JD006156.
- Johns, T. C., and Coauthors, 2006: The new Hadley Centre climate model (HadGEM1): Evaluation of coupled simulations. *J. Climate*, **19**, 1327–1353.
- Johnson, R. H., and D. L. Priegnitz, 1981: Winter monsoon convection in the vicinity of north Borneo. Part II: Effects on large-scale fields. *Mon. Wea. Rev.*, **109**, 1615–1628.
- Joyce, R. J., J. E. Janowiak, P. A. Arkin, and P. Xie, 2004: CMORPH: A method that produces global precipitation estimates from passive microwave and infrared data at high spatial and temporal resolution. *J. Hydrometeorol.*, **5**, 487–503.
- Kalnay, E., and Coauthors, 1996: The NCEP/NCAR 40-Year Reanalysis Project. *Bull. Amer. Meteor. Soc.*, **77**, 437–471.
- Keenan, T., and Coauthors, 2000: The Maritime Continent Thunderstorm Experiment (MCTEX): Overview and some results. *Bull. Amer. Meteor. Soc.*, **81**, 2433–2455.
- Kiehl, J. T., J. J. Hack, G. B. Bonan, B. A. Boville, D. L. Williamson, and P. J. Rasch, 1998: The National Center for Atmospheric Research Community Climate Model (CCM3). *J. Climate*, **11**, 1307–1326.
- Kitada, T., and K. Igarashi, 1986: Numerical analysis of air pollution in a combined field of land/sea breeze and mountain/valley wind. *J. Climate Appl. Meteor.*, **25**, 767–784.
- Kummerow, C., and Coauthors, 2000: The status of the Tropical Rainfall Measuring Mission (TRMM) after two years in orbit. *J. Appl. Meteor.*, **39**, 1965–1982.
- Lorenz, P., and D. Jacob, 2005: Influence of regional scale information on the global circulation: A two-way nesting climate simulation. *Geophys. Res. Lett.*, **32**, L18706, doi:10.1029/2005GL023351.
- Mapes, B. E., T. T. Warner, and M. Xu, 2003: Diurnal patterns of rainfall in northwestern South America. Part III: Diurnal gravity waves and nocturnal convection offshore. *Mon. Wea. Rev.*, **131**, 830–844.
- Mori, S., and Coauthors, 2004: Diurnal land–sea rainfall peak migration over Sumatra island, Indonesian Maritime Continent, observed by TRMM satellite and intensive rawinsonde soundings. *Mon. Wea. Rev.*, **132**, 2021–2039.
- Neale, R., and J. Slingo, 2003: The Maritime Continent and its role in the global climate: A GCM study. *J. Climate*, **16**, 834–848.
- Nesbitt, S. W., and E. J. Zipser, 2003: The diurnal cycle of rainfall and convective intensity according to three years of TRMM measurements. *J. Climate*, **16**, 1456–1475.
- Nitis, T., D. Kitsou, Z. B. Klaic, M. T. Prtenjak, and N. Mousiopoulos, 2005: The effects of basic flow and topography on the development of the sea breeze over a complex coastal environment. *Quart. J. Roy. Meteor. Soc.*, **131**, 305–327.
- Pal, J. S., E. E. Small, and E. A. B. Eltahir, 2000: Simulation of regional scale water and energy budgets: Representation of subgrid cloud and precipitation processes within RegCM. *J. Geophys. Res.*, **105**, 29 579–29 594.
- Pielke, R. A., 1974: A three-dimensional numerical model of the sea breezes over south Florida. *Mon. Wea. Rev.*, **102**, 115–139.
- Prandtl, L., 1952: *Essentials of Fluid Mechanics*. Blakie and Son, 451 pp.
- Qian, J.-H., F. H. M. Semazzi, and J. S. Scroggs, 1998: A global nonhydrostatic semi-Lagrangian atmospheric model with orography. *Mon. Wea. Rev.*, **126**, 747–771.
- , F. Giorgi, and M. S. Fox-Rabinovitz, 1999: Regional stretched grid generation and its application to the NCAR RegCM. *J. Geophys. Res.*, **104**, 6501–6513.
- Ramage, C. S., 1968: Role of a tropical “maritime continent” in the atmospheric circulation. *Mon. Wea. Rev.*, **96**, 365–370.
- Rampanelli, G., D. Zardi, and R. Rotunno, 2004: Mechanisms of up-valley winds. *J. Atmos. Sci.*, **61**, 3097–3111.
- Riehl, H., 1954: *Tropical Meteorology*. McGraw-Hill, 392 pp.
- , and J. S. Malkus, 1958: On the heat balance in the equatorial trough zone. *Geophysica*, **6**, 503–538.
- Roeckner, E., and Coauthors, 1996: The atmospheric general circulation model ECHAM4: Model description and present-day climate. Max-Planck-Institut für Meteorologie Rep. 218, Hamburg, Germany, 90 pp.
- Saito, K., T. Keenan, G. Holland, and K. Puri, 2001: Numerical simulation of the diurnal evolution of tropical island convection over the Maritime Continent. *Mon. Wea. Rev.*, **129**, 378–400.
- Sato, T., 2004: The current status of the Earth Simulator. *J. Earth Simulator*, **1**, 6–7.
- Semazzi, F. H. M., J.-H. Qian, and J. S. Scroggs, 1995: A global nonhydrostatic semi-Lagrangian atmospheric model without orography. *Mon. Wea. Rev.*, **123**, 2534–2550.
- Simpson, J., N. E. Westcott, R. J. Clerman, and R. A. Pielke, 1980: On cumulus mergers. *Arch. Meteor. Geophys. Bioklim.*, **29A**, 1–40.
- , T. D. Keenan, B. Ferrier, R. H. Simpson, and G. J. Holland, 1993: Cumulus merger in the Maritime Continent region. *Meteor. Atmos. Phys.*, **51**, 73–99.
- Simpson, J. E., 1996: Diurnal changes in sea-breeze direction. *J. Appl. Meteor.*, **35**, 1166–1169.
- Tao, W.-K., and Coauthors, 2006: Retrieval of latent heating from TRMM measurements. *Bull. Amer. Meteor. Soc.*, **87**, 1555–1572.
- Trenberth, K. E., 1999: Atmospheric moisture recycling: Role of advection and local evaporation. *J. Climate*, **12**, 1368–1381.
- Wai, M. M.-K., P. T. Welsh, and W.-M. Ma, 1996: Interaction of secondary circulations with the summer monsoon and diurnal rainfall over Hong Kong. *Bound.-Layer Meteor.*, **81**, 123–146.
- Webster, P. J., C. A. Clayson, and J. A. Curry, 1996: Clouds, radiation, and the diurnal cycle of the sea surface temperature in the tropical western Pacific. *J. Climate*, **9**, 1712–1730.
- Wyrki, K., 1973: An equatorial jet in the Indian Ocean. *Science*, **181**, 262–264.
- Xie, P., and P. A. Arkin, 1996: Analysis of global monthly precipitation using gauge observations, satellite estimates, and numerical model predictions. *J. Climate*, **9**, 840–858.
- Yang, G.-Y., and J. Slingo, 2001: The diurnal cycle in the Tropics. *Mon. Wea. Rev.*, **129**, 784–801.